ADVANCED OPTICAL MATERIALS
www.advopticalmat.de

Check for updates

Slide-Ring Supramolecular Mechanoresponsive Elastomer with Reversible Luminescence Behavior

*Yi Zhang, Yong Chen, Hui Zhang, Lei Chen, Qiyu Bo, and Yu Liu**

A solid slide-ring supramolecular elastomer is constructed by free-radical polymerization of 2-(2-methoxyethoxy)ethyl methacrylate, acrylate-modified perylene diimides (PDI), and the polyrotaxane (PR) cross-linker. Benefiting from reciprocating shuttle function of slide-ring PR formed by acrylate-modified α-cyclodextrin threading on polyethylene glycol, the resultant supramolecular elastomer not only presents excellent tensile property, toughness, and fatigue resistance up to 100 cycles, but also gives reversible mechano-induced fluorescence changes from red to orange luminescence due to a reversible conversion of PDI dimer to monomer upon mechanical stretching. After the dye molecule Nile blue is added as a fluorescent acceptor, the supramolecular elastomer exhibits highly reversible mechano-induced regulation of energy transfer and can perform five cycles without optical fatigue. This bifunctional mechanochromic slide-ring supramolecular elastomer, which not only possesses mechanically reversible motion of the slide-ring cross-linkers but also has the mechanochromic response of fluorophore, endows the intrinsic superiority of slide-ring into fatigue resistant mechanoresponsive strain sensing materials.

1. Introduction

The slide-ring system formed by macrocycles threading on polymers has attracted more and more attention due to its unique dynamic mechanical interlocking structure[1] and is widely applied in the fields of electrode binder,[2] flexible electronics,[3] 3D printing materials,[4] and stimuli-responsive smart system[5] in recent years. Different from the covalent polymer,[6] the supramolecular slide-ring system maintains the polymer structural integrity and recoverability through the free movement of cross-linked macrocyclic molecules on the polymer chain over a large range under exogenous forces. Therefore, this dynamic slide-ring network structure can support the repeated triggering of response and the reversible transmission of the signal to achieve specific functions (such as sensing, feedback, self-healing, etc.), which plays a crucial role in the development of intelligent soft materials with excellent mechanical properties.[7] For example, Ito et al. reported the slide-ring supramolecular hydrogel formed by the cross-linking of low-coverage polyrotaxanes (PR), showing the good mechanical property because the sliding of cross-linking sites on polymer chains could efficiently relieve the stress in the system.[1] In addition, they prepared the transparent supramolecular elastomer with enhanced mechanical properties (such as stiffness and toughness) via the PR cross-linker.[8] We reported the slide-ring hydrogel with good mechanical properties formed by the copolymerization of acrylamide and the rotaxane cross-linker composed of α-cyclodextrin (α-CD) and polyethylene glycol diacrylate (PEG), which was applied in stretchable supercapacitors and flexible electronic devices.[9] Except for the polymers with slide-ring cross-linkers to form the reversible mechanical responsive dynamic network,[10] the polymer that covalently introduces mechanoresponsive fluorophores can also construct the mechanochromic system.

It is well known that the mechanochromic system can adapt to exogenous mechanical forces and respond sensitively and macroscopically, exhibit the optical absorption and/or luminescence characteristics change, and are widely used in the smart sensing system[11] and biomimetic flexible materials.[12] Mechanochromic systems typically integrate force-responsive active sites and dynamic network structures that response to achieve the synergistic optimization of sensory performance.[13] Most of the mechanoresponsive active sites are based on the irreversible cleavage of covalent bonds, which limits the reversibility of responses as their reformation is kinetically or thermodynamically inhibited.[14] Therefore, the response sites based on supramolecular noncovalent interactions (e.g., host–guest interactions,[15] charge transfer interactions,[16] π–π interactions,[17]

Y. Zhang, Y. Chen, H. Zhang, L. Chen, Y. Liu
College of Chemistry
State Key Laboratory of Elemento-Organic Chemistry
Nankai University
Tianjin 300071, P. R. China
E-mail: yuliu@nankai.edu.cn
Y. Chen, Y. Liu
Collaborative Innovation Center of Chemical Science and Engineering (Tianjin)
Nankai University
Tianjin 300071, P. R. China
Y. Chen, Y. Liu
Haihe Laboratory of Sustainable Chemical Transformations
Tianjin 300071, P. R. China
Q. Bo
Institute of Modern Optics, Nankai University
Tianjin Key Laboratory of Micro-scale Optical Information Science and Technology
Tianjin 300350, China
The ORCID identification number(s) for the author(s) of this article can be found under https://doi.org/10.1002/adom.202202828.

DOI: 10.1002/adom.202202828

 © 2023 Wiley-VCH GmbH

21951071, 0, Downloaded from https://onlinelibrary.wiley.com/doi/10.1002/adom.202202828 by Nankai University, Wiley Online Library on [10/02/2023]. See the Terms and Conditions (https://onlinelibrary.wiley.com/terms-and-conditions) on Wiley Online Library for rules of use; OA articles are governed by the applicable Creative Commons License

and dissociation of metal–ligand interactions[18]) become new design choices for the construction of reversible real-time macroscopic feedback mechanochromic artificial materials. For example, Schrettl et al. reported the supramolecular mechanophore motif consisting of two perylene diimide (PDI) molecules covalently linked via a short linker and covalently introduced into the poly(methyl methacrylate) chain to form a mechanoresponsive polymer.[19] The change of intramolecular π–π interactions among PDIs in the polymer leads to the conversion of excimer emission in the force-free state to the monomeric fluorescence under the mechanical force. Brighenti et al. constructed a self-diagnostic poly(dimethylsiloxane) elastomer.[20] It comprised a fluorescence-silenced supramolecular detection probe formed by a host–guest complex, where the guest molecule pyrene conjugated N-methylpyridinium salt and the host molecule calixarene derivative. Applying stress to elastomers disrupted host–guest interactions and enabled the identification of polymer strain intensity by the fluorescence detection. Although a number of mechanoresponsive luminescent materials based on supramolecular noncovalent interactions are documented, the bifunctional mechanochromic slide-ring supramolecular elastomer, which not only possesses mechanically reversible motion of PR slide-ring cross-linkers but also has the mechanochromic response of fluorophore is rarely reported so far to the best of our knowledge. Herein, we report several mechanochromic supramolecular elastomers (**Scheme 1**) copolymerized from 2-(2-methoxyethoxy)ethyl methacrylate (MEMA), the mechanoresponsive group acrylate-modified PDI derivative **1**, and PR cross-linker formed by acrylate-modified α-CD threading on PEG and end-capped with adamantine stoppers. The improved mechanical properties (fracture stress, elastic modulus, toughness, fatigue resistance up to 100 cycles) and reversible mechanochromism of these supramolecular elastomers are attributed to the force-responsive active sites and slide-ring dynamic network structure based on supramolecular interactions. Then, Nile blue (NiB) as the energy acceptor is doped into the supramolecular system. By affecting the spectral matching degree between the energy donor and the acceptor, the energy transfer (ET) efficiency could be reversibly controlled through the mechanical force, and the mechanical induction regulation of ET efficiency with the excellent fatigue resistance is achieved.

2. Results and Discussion

As the slide-ring cross-linker, the PR was synthesized by threading acrylate-modified α-CD on PEG and end-capped with adamantine stoppers.[8,10a] According to the calculation based on peak areas of the ^{1}H NMR spectrum (Figure S1, Supporting Information), there are ≈91.7 CD units threaded onto a PEG chain ($M_w \approx 35\,000$) by comparing the H1 protons of α-CD at 4.80 ppm (one α-CD unit has 6 H1 protons) and the methylene protons of PEG at 3.50 ppm (a molecule of PEG chain has 3182 methylene protons), and the coverage yield of the PEG chain is calculated to be 23%. In order to improve the water solubility of PR and provide cross-linking functional sites, we randomly modified hydroxypropyl groups onto CD through the substitution reaction of CD hydroxyl groups with epoxy propane, and further modified acrylate groups to CD through the addition reaction of 2-acryloylethyl isocyanate with CD hydroxyl groups. The average numbers of these two functional groups on CD are estimated to be 2.8 and 1.5, respectively, by comparing the H1 protons of α-CD at 4.80 ppm with the methyl protons of

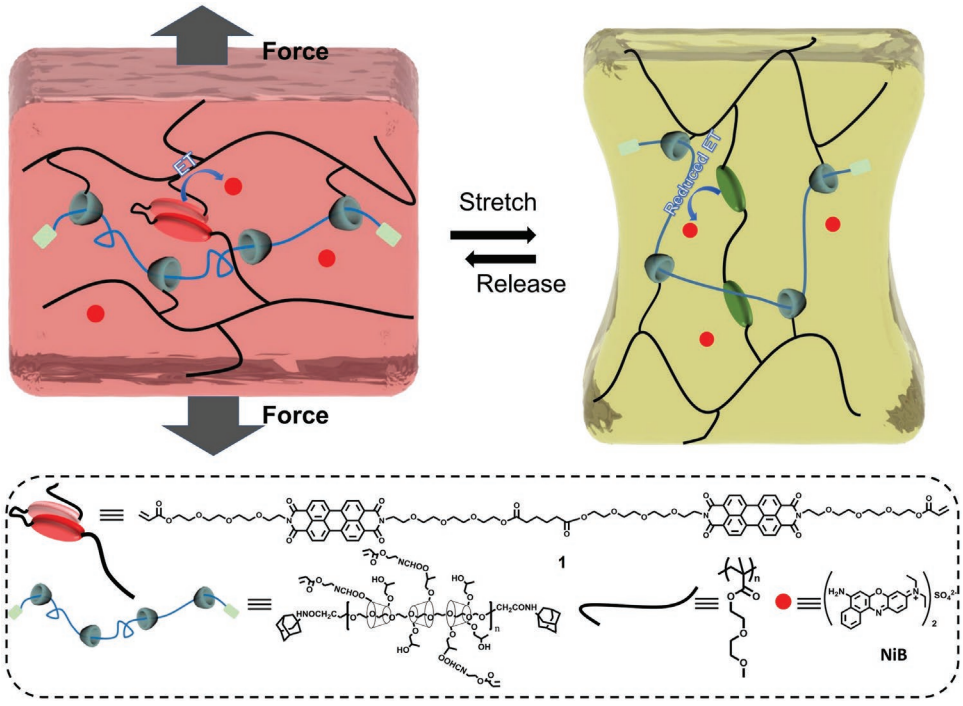

Scheme 1. Schematic illustration of mechanoresponsive slide-ring supramolecular elastomer.

© 2023 Wiley-VCH GmbH

21951071, 0, Downloaded from https://onlinelibrary.wiley.com/doi/10.1002/adom.202202828 by Nankai University, Wiley Online Library on [10/02/2023]. See the Terms and Conditions (https://onlinelibrary.wiley.com/terms-and-conditions) on Wiley Online Library for rules of use; OA articles are governed by the applicable Creative Commons License

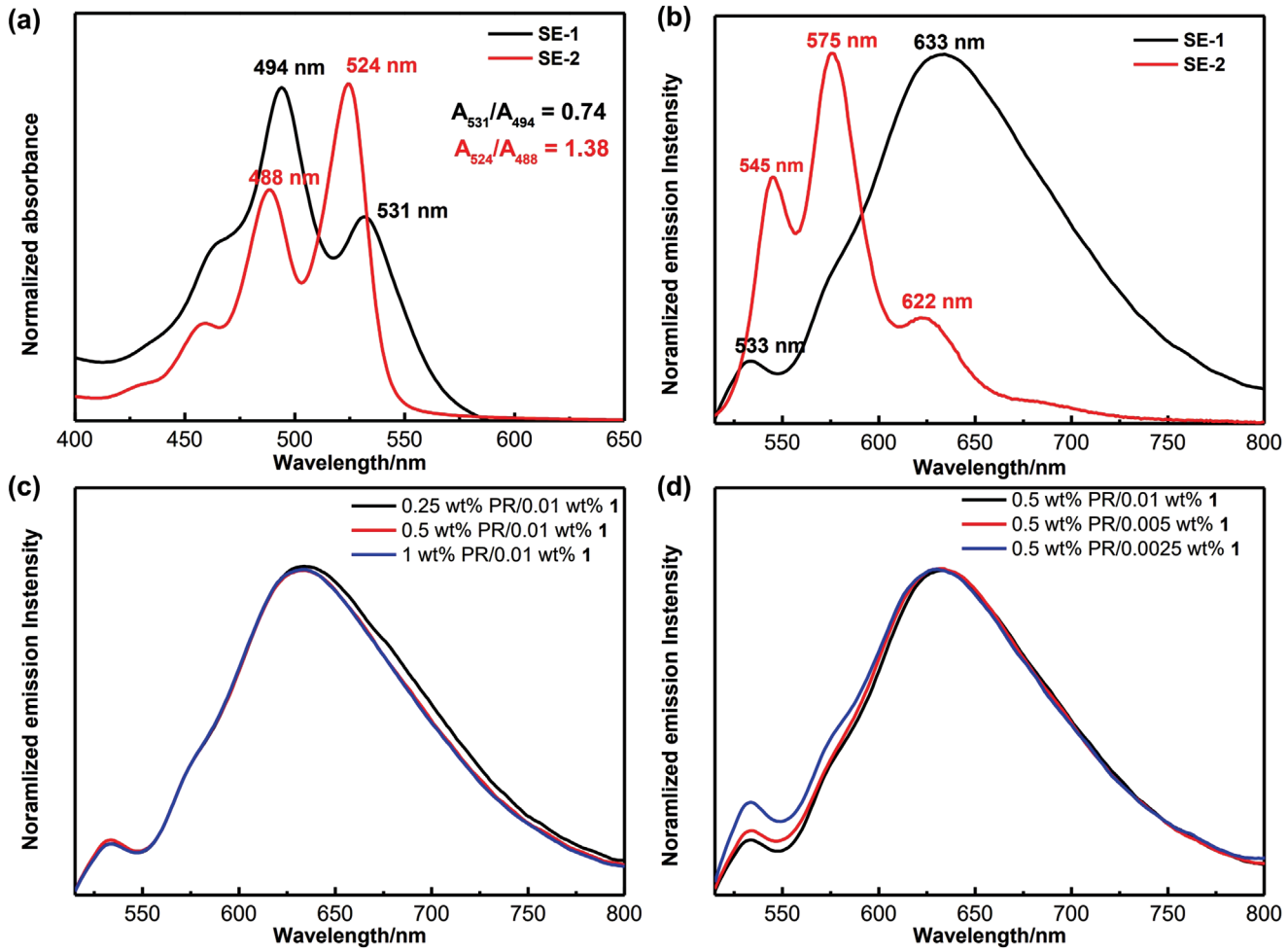

Figure 1. a) UV-vis absorption spectra and b) fluorescence emission spectra of supramolecular elastomers **SE-1** and **SE-2** (λ_{ex} = 494 nm). c) The fluorescence emission spectra of elastomers with different cross-likers (λ_{ex} = 494 nm, fixed **1** as 0.01 wt%). d) Fluorescence emission spectra of supramolecular elastomers with different mass fractions of **1** (λ_{ex} = 494 nm, fixed PR as 0.5 wt%).

hydroxypropyl groups at 1.05 ppm as well as the protons of acrylate groups at 6.33 ppm. The force-responsive acrylate-modified PDI derivative **1** and a reference molecule acrylate-modified PDI-monomer **2** were also synthesized (Scheme S1, Supporting Information), and the ^{1}H NMR, ^{13}C NMR, and high-resolution mass spectrometry results proved that they were successfully obtained (Figures S2–S7, Supporting Information).

In order to study the photophysical behavior of the supramolecular elastomer, we first investigated the UV-vis absorption and fluorescence spectra of **1** and **2** in dichloromethane (DCM) solution. As shown in Figure S8a in the Supporting Information, the characteristic absorption peak intensity ratios of PDI were 0.84 for **1** and 1.60 for **2**, respectively. By using the reported equation (Supporting Information Equation (S1)), the calculated proportion of folded dimer in **1** was 87.4%, indicating that most of **1** occurred the intramolecular folding to form PDI dimer, while **2** had almost no intermolecular aggregation at 5 µmol L^{-1} in DCM solution.[17b,19] When 0.01 wt% mass fraction **1** or **2** was added, supramolecular elastomers **SE-1** or **SE-2** (Tables S1 and S2, Supporting Information) were, respectively, obtained by copolymerization with MEMA and 0.5 wt% PR cross-linker (relative to the monomer MEMA). In the UV-vis absorption of elastomers, two main absorption peaks of PDI in **SE-1** red-shifted to 494 and 531 nm, respectively, compared with those in the solution state. **SE-2** showed the similar phenomenon, where absorption peaks of PDI red-shifted to 488 and 524 nm, respectively (**Figure 1**a). The characteristic absorption peak intensity ratios of PDI were 0.74 for **SE-1** and 1.38 for **SE-2**, respectively, indicating that **1** still mostly formed the folded dimers, and the supramolecular elastomer network enhanced the folded dimers, while **2** existed as monomers. The fluorescence spectrum (Figure S8b, Supporting Information) also reflected the difference in the folding degree of **1** and **2** in solution. **1** showed a significantly enhanced emission band at 628 nm, which belonged to the dimer emission of the spontaneous folded PDI dimer. In addition, **1** showed orange-red fluorescence, but **2** showed green fluorescence, under 365 nm UV light, as shown in the photographs inserted in Figure S8b in the Supporting Information. As expected, **SE-1** mainly exhibited a broad band of dimers at 633 nm, and the monomer band at 533 nm was relatively weak. The maximum emission bank of **SE-2** exhibited the bright green emission and the main band at 575 nm

© 2023 Wiley-VCH GmbH

21951071, 0, Downloaded from https://onlinelibrary.wiley.com/doi/10.1002/adom.202202828 by Nankai University, Wiley Online Library on [10/02/2023]. See the Terms and Conditions (https://onlinelibrary.wiley.com/terms-and-conditions) on Wiley Online Library for rules of use; OA articles are governed by the applicable Creative Commons License

(Figure 1b). The UV-vis absorption and fluorescence spectra of **1** and **2** at a series of diluted concentrations (Figures S9–S16, Supporting Information) also demonstrated that **1** could form stable, highly folded dimers independent on concentration. However, **2** existed as monomers at a lower concentration. With the increase of concentration, **2** aggregated to form dimers, and its existence form was greatly affected by the concentration. The same phenomena were also observed in the elastomer matrix. The value of A_{531}/A_{494} reflected in the UV absorption spectrum showed that **1** existed as folded dimers in the elastomer, and the proportion of dimers increased with the increased concentration of **1**. The change of UV absorption A_{524}/A_{488} indicated that **2**'s dimers would gradually form at a relatively high concentration of **2** in the elastomer (Figure S17, Supporting Information). The above experimental results indicated that **1** tended to form a stable dimer with the excimer emission in diluted solution and elastomer, and the luminescence of dimer and monomer molecules were distinctly different. In addition, the mass fraction of PR hardly affected the emission of **1** in the fluorescence spectrum of the elastomer (Figure 1c), and this result was also reflected in the elastomer with various mass fractions of **1** (Figure S18, Supporting Information). From the fluorescence emission spectrum of supramolecular elastomers with different mass fractions of **1** (Figure 1d), it could be concluded that the high mass fraction of **1** in the elastomer could promote the emission of PDI dimers. It is well known that the π–π interactions between dimer molecules could be destroyed and restored reversibly under the certain external forces. These results indicate that **1** provides excellent light-emitting primitives for mechanochromic materials.

Then, we investigated the mechanical property of the elastomer. **Figure 2**a–c illustrates the stress-stretch ratio curves and the derived mechanical parameters of the elastomer containing **1** prepared by the traditional cross-linker 2-(2-methoxyethoxy) ethyl methacrylate and different proportions of PR cross-linker, respectively (the repeated experiment results are shown in Figure S19, Supporting Information). The fracture strains and stresses of the PR supramolecular elastomer were larger than those of the traditional cross-linker elastomer in Figure 2a. It is worth noting that supramolecular elastomers exhibit strain-hardening behavior. As can be seen from the stress–strain diagram, after the yield region, the slope of the curve increased, and the modulus and strength increased significantly, indicating that the sample became stiffer. The possible reason for

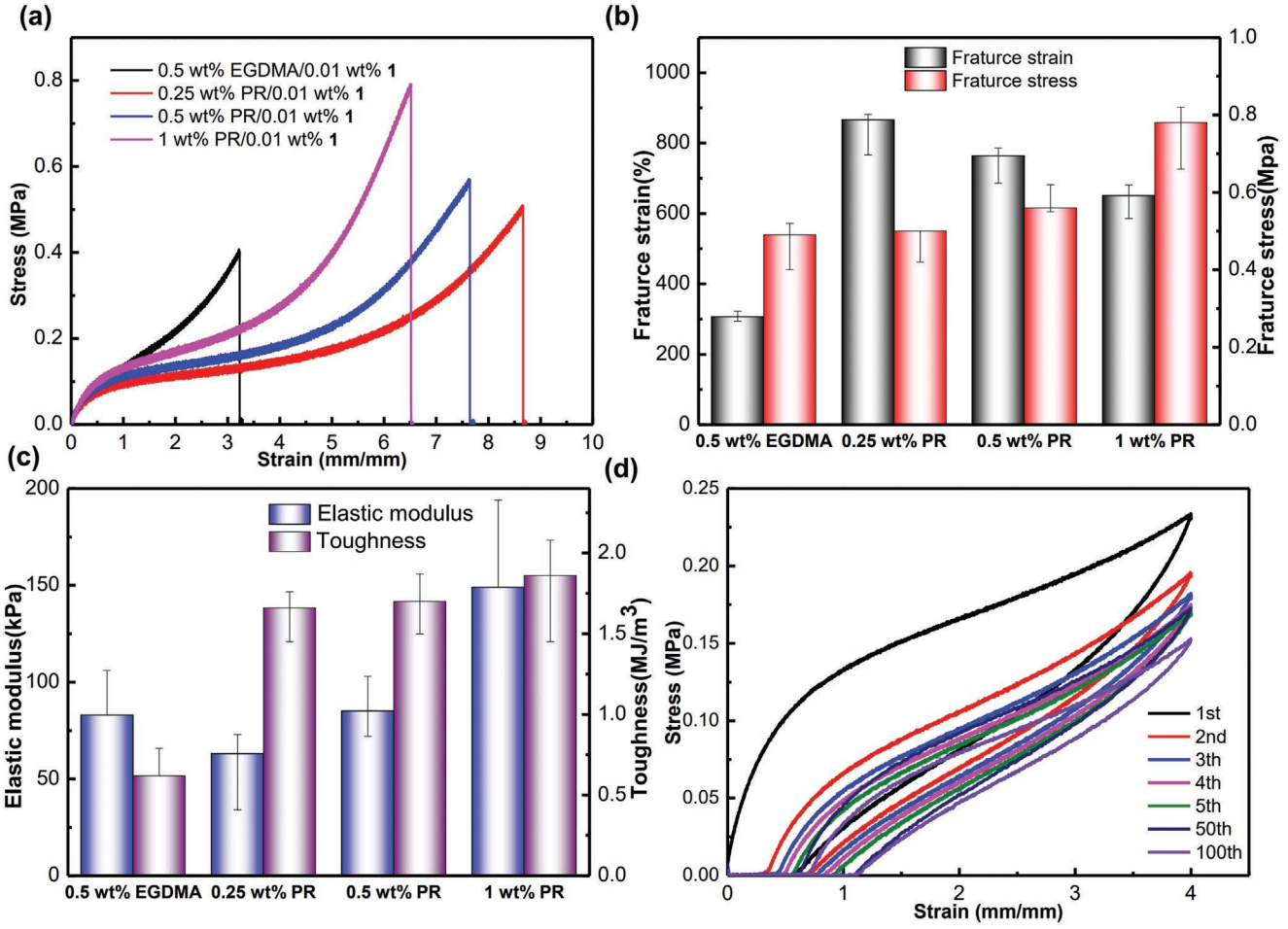

Figure 2. Mechanical properties of elastomers with traditional cross-linkers and different ratios of PR cross-linkers. a) Tensile stress–strain curves. b) The fracture stresses and strains. c) Elastic moduli and toughness. d) The cyclic hysteresis loops of the stress-extension ratio curves of supramolecular elastomers (0.5 wt% PR/0.01 wt% **1**).

© 2023 Wiley-VCH GmbH

21951071, 0, Downloaded from https://onlinelibrary.wiley.com/doi/10.1002/adom.202202828 by Nankai University, Wiley Online Library on [10/02/2023]. See the Terms and Conditions (https://onlinelibrary.wiley.com/terms-and-conditions) on Wiley Online Library for rules of use; OA articles are governed by the applicable Creative Commons License

21951071, 0, Downloaded from https://onlinelibrary.wiley.com/doi/10.1002/adom.202202828 by Nankai University, Wiley Online Library on [10/02/2023]. See the Terms and Conditions (https://onlinelibrary.wiley.com/terms-and-conditions) on Wiley Online Library for rules of use; OA articles are governed by the applicable Creative Commons License

the improved mechanical property of supramolecular elastomers is that PR could provide slidable cross-linking sites, which enabled the reversible movement of the cross-linked CD along PEG chains and led to efficient energy dissipation during stretching. In supramolecular elastomers, with increasing PR mass (from 0.25 to 1 wt%), the fracture stress, elastic modulus, and toughness increased from 0.50 to 0.78 MPa, 63 to 149 kPa, and 1.66 to 1.86 MJ m^{-3}, respectively. However, the fracture strain exhibited the opposite phenomenon, decreasing from 866% to 651% with the increase of PR (Figure 2c,d). This is attributed to the fact that the increase of the amount of slidering cross-linking agent PR leads to an increase of the cross-linking density and strength, which also leads to the increased brittleness and the decreased elongation at breaking of the elastomer. Therefore, the supramolecular elastomer with 0.5% PR showed good mechanical parameters, such as 764% fracture strain, 0.56 MPa fracture stress, 85 kPa elastic modulus, and 1.70 MJ m^{-3} toughness. The cyclic hysteresis loops of stress-extension ratio curves showed that the supramolecular elastomer also had good fatigue resistance. Even if it was cyclically stretched for 100 times, the elastomer still had a certain degree of recovery (Figure 2d). That is, they could almost recover to the original length in an unstressed state for a period of time, which enabled the fatigue resistance of the mechanochromic response. Significantly, elastomers with different PR contents all had this recovery property (Figure S20, Supporting Information). Supramolecular elastomers with different mass fractions of **1** exhibited similar elongation at breaking (Figure S21, Supporting Information), indicating that the content of **1** hardly affected the tensile property of elastomers, probably due to their relatively less content compared to that of PR. Furthermore, we investigated the thermal property of elastomers. The differential scanning calorimetry curves showed that traditional elastomers and supramolecular elastomers **SE-1** had similar glass transition temperatures around −47 °C (Figure S22, Supporting Information). In the thermogravimetric curves results, the elastomers remained stable without weight loss below 150 °C under nitrogen conditions, demonstrating that they had good thermal stability (Figure S23, Supporting Information). The weight of elastomers decreased sharply at around 350 °C, meaning that the weight loss rate reached the maximum (Figure S24, Supporting Information). Benefiting from the stability of polyrotaxane topological structure, thermal and solvent treatment would not destroy the host–guest interaction of CD and PEG, and thus would not affect the crystallinity of cyclodextrins on polyrotaxane. Therefore, different thermal and solvent treatments would not affect the mechanical properties of the supramolecular elastomer as shown in Figure S25 in the Supporting Information.

Great mechanical properties are the basis of mechanical mechanochromic. The elastomer with 0.5 wt% PR cross-linkers and 0.01 wt% **1** (i.e., **SE-1**) was used to investigate its mechanical mechanochromic property. The supramolecular elastomer containing the mechanochromic molecule **1** displayed a visible fluorescence color change upon bulk deformation. As shown in **Figure 3**a, when the deformation varied from 0% to 700%, the luminescence of **SE-1** changed from red to orange, which could be clearly observed by the naked eye, under 365 nm UV light (Movie S1, Supporting Information). In situ fluorescence measurements of **SE-1** were monitored under different strains (Figure 3b). With the increase of strain, the intensity ratio of fluorescence peaks at 533 or 578 nm to that of the PDI dimer at 633 nm was increased, indicating that a part of folded dimers transformed into a monomer state during the stretching process. In other words, the large deformation increased the intermolecular distance of PDI dimers, which disrupted the π–π interaction between PDIs and led to the enhanced luminescence of the monomer. The coordinates on the corresponding Commission Internationale de l'Éclairage (CIE) of **SE-1** were also changed from the red to the orange region under strains (Figure 3c), which was also consistent with the color change shown in the photos. Then, we investigated the alternating reciprocating fluorescence spectra of 100% and 400% strains (Figure 3d), the results demonstrated that the fluorescence emission of the system was mechanically reversible, and the macroscopic mechanochromic process could be repeated many times without obvious force fatigue and luminescence fatigue. Those all benefited from the good reversible interaction of two supramolecular forces in the system: the good mechanical properties endowed by the host–guest interactions of PR and the mechanochromic behavior endowed by the π–π interactions of PDIs. As a comparison, we recorded the photos of **SE-2** stretched to different deformations. As can be seen in Figure S26 in the Supporting Information, **SE-2** emitted the green fluorescence under 365 nm illumination, and there was no obvious color change after deformation. These also further suggested that the reversible formation and destruction of PDI dimers in **SE-1** was the main reason causing the mechanochromicity.

To explore the mechanical force-regulated ET, NiB as an energy acceptor was introduced into **SE-1**. **Figure 4**a shows that the fluorescence emission spectrum of **SE-1** overlapped the UV absorption spectrum of NiB very well, indicating that ET could occur from **SE-1** to NiB. The NiB fluorescence emission of the elastomer at 678 nm decreased and blue-shifted with increasing strain, meanwhile the fluorescence banks of **SE-1** at 533 and 578 nm increased (Figure 4b). This result indicated that different strains could change the efficiency of ET. Changes of ET efficiency were achieved due to stretching altering the fluorescence emission of **SE-1** and changing the degree of spectral overlap between donor and acceptor. The reversible fluorescence spectra of **SE-1**/NiB under 100% and 400% strains showed that the mechano-regulated ET had good reversibility (Figure 4c). Furthermore, the comparison of fluorescence intensities of **SE-1**/NiB at 533 and 670 nm upon the repeated 100% and 400% strain stretching processes showed that the fluorescence intensity could be completely recovered. Crucially, the above energy transfer switching process was repeated five times without obvious decay, showing the good antifatigue performance (Figure 4d). As shown in Figure S27 in the Supporting Information, under 365 nm UV light irradiation, the visible force-regulated ET luminescence of **SE-1**/NiB with different strains changed from red to orange, which was consistent with the change of CIE coordinates. Moreover, the tensile stress–strain curve of **SE-1** with different NiB concentrations indicated that the addition of NiB hardly affected the mechanical property of supramolecular elastomers because the content of NiB in the elastomer was very low (Figure S28, Supporting Information).

 © 2023 Wiley-VCH GmbH

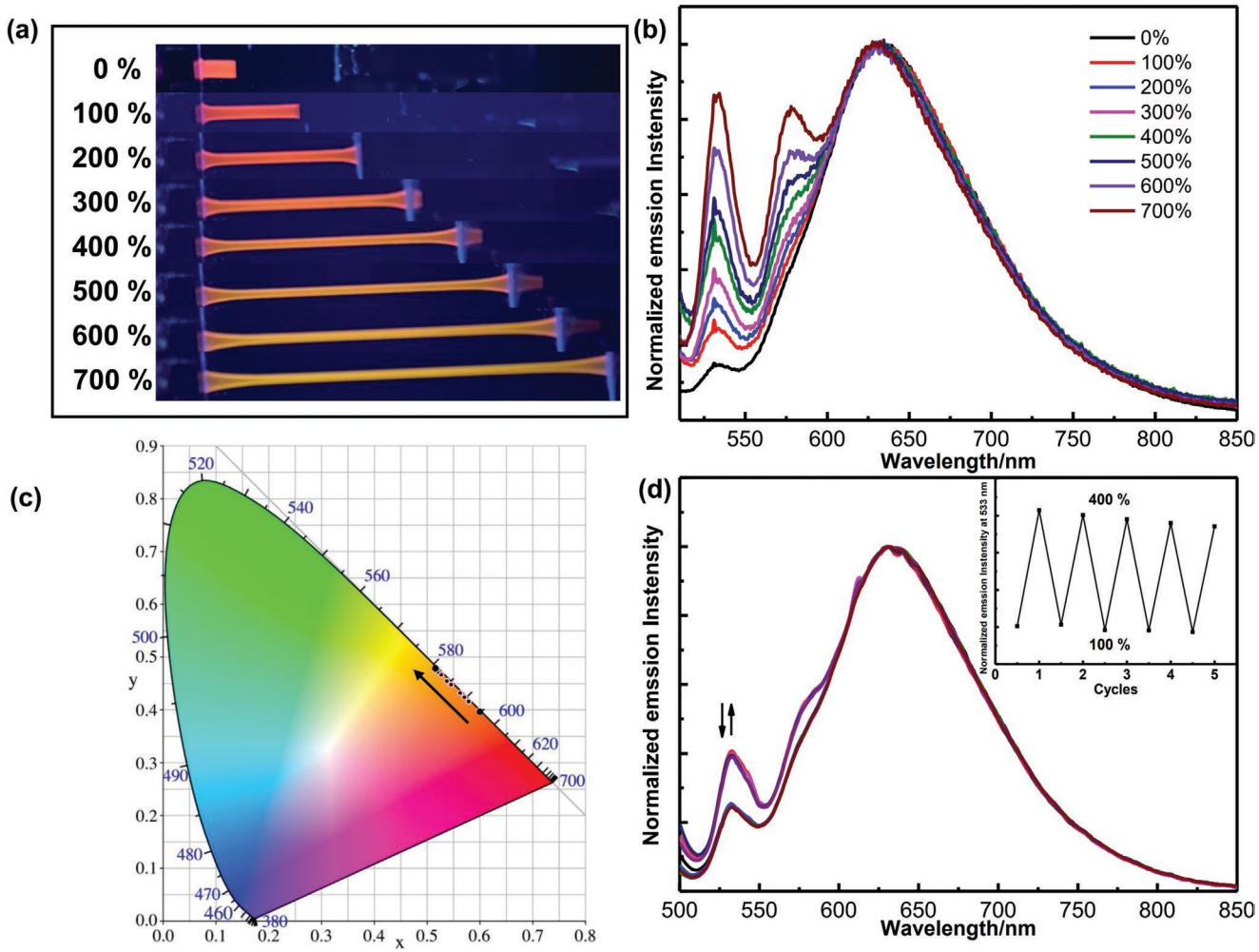

Figure 3. a) Photographs of the **SE-1** with different strain under UV light (λ_{ex} = 365 nm). b) Fluorescence spectrum of **SE-1** under different strain during the tensile (λ_{ex} = 470 nm). c) CIE chromaticity diagram of **SE-1** under different strain excited by 470 nm. d) The reversibility of fluorescence switching of **SE-1** under 100% and 400% strain (Inset: The fluorescence intensity changes at 533 nm of **SE-1** upon alternating 100% and 400% strain; λ_{ex} = 470 nm).

In addition, elastomers **SE-1** with different concentrations of NiB all have mechanochromic fluorescence behavior as shown in Figure S29 in the Supporting Information. However, the low concentration (0.002 wt%) of NiB led to the low ET efficiency, and the high concentration (0.006 wt%) of NiB led to the low regulation effect, which were not conducive to the mechanical force-regulated ET behavior. Control experiments showed that the NiB fluorescence in SE-NiB (0.5 wt% PR/0.004 wt% NiB) elastomer was very weak when excited by 470 nm, while the significant fluorescence emission could be observed in **SE-1**/NiB system under the same experimental conditions, indicating that ET from **SE-1** to NiB is effective (Figure S30, Supporting Information). Another evidence of efficient ET was the change of the time-resolved photoluminescence decay curve before and after the addition of acceptor molecules (Figure S31, Supporting Information), the fluorescence lifetime of **SE-1**/NiB at 633 nm decreased after the addition of NiB, and the fluorescence lifetime at 675 nm increased compared to those of free-NiB. These further confirmed that the mechano-induced regulation was based on the change of ET efficiency. This good reversible modulation of ET illustrates the key role of slide-ring cross-linkers in mechanoresponsive systems.

3. Conclusion

In summary, the bifunctional mechanochromic slide-ring supramolecular elastomer, which not only possesses the mechanical reversibility of the slide-ring PR but also has the mechanochromic response of fluorophore, is constructed by free-radical polymerization with acrylate-modified PDI **1** as mechanoresponsive active sites, slide-ring PR cross-linker comprising PEG threads and acrylate-modified a-CD rings, and MEMA monomers. Owing to the inherent long-distance reversible sliding motion characteristics of slide-ring PR cross-linkers and reversible dimer to monomer conversion of PDI molecule, the supramolecular elastomers not only possess improved mechanical properties (such as fracture strain, toughness, and fatigue resistance), but also are endowed with highly reversible mechanoresponsive fluorescence changes, ultimately

© 2023 Wiley-VCH GmbH

21951071, 0, Downloaded from https://onlinelibrary.wiley.com/doi/10.1002/adom.202202828 by Nankai University, Wiley Online Library on [10/02/2023]. See the Terms and Conditions (https://onlinelibrary.wiley.com/terms-and-conditions) on Wiley Online Library for rules of use; OA articles are governed by the applicable Creative Commons License

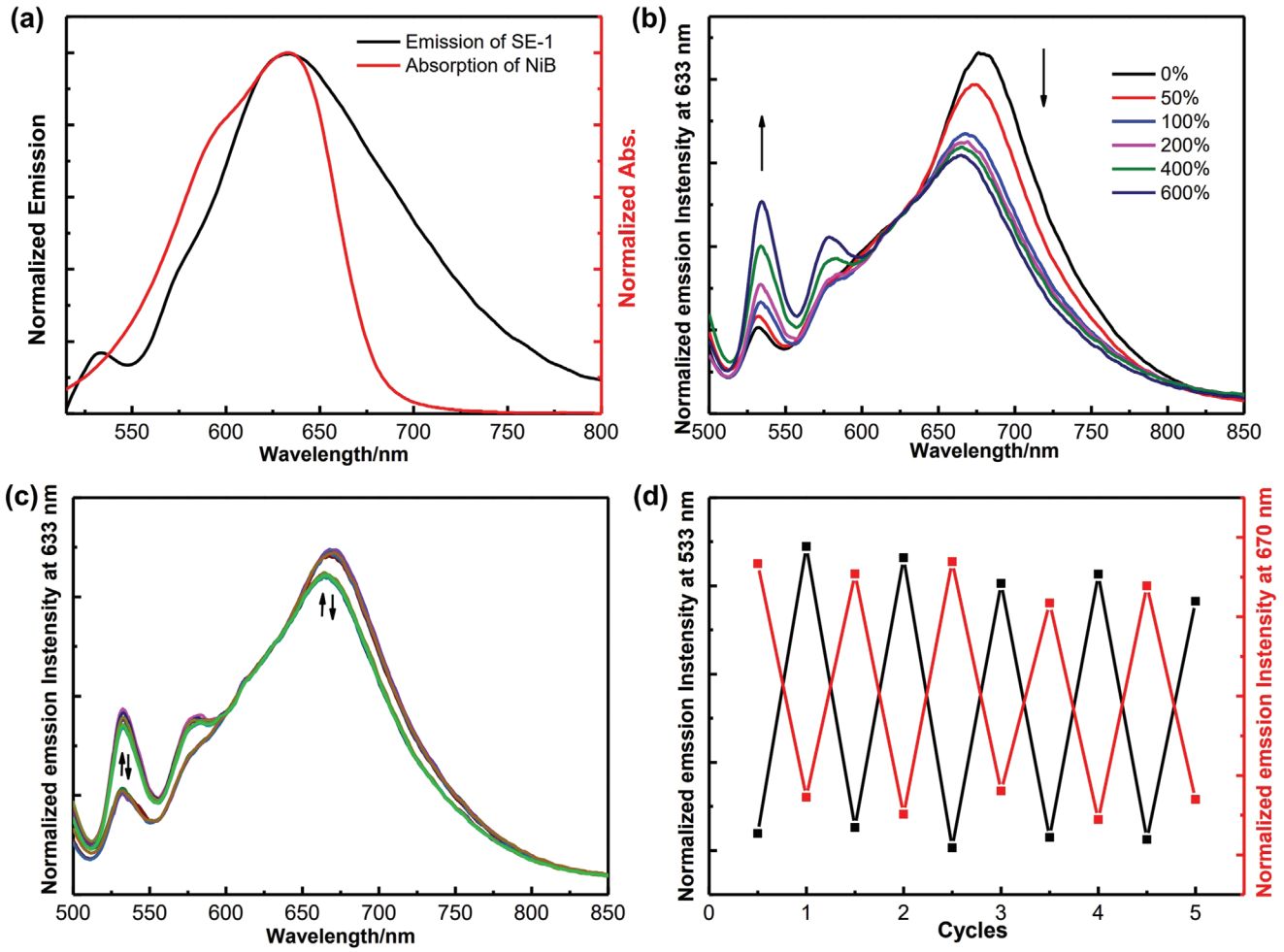

Figure 4. a) Normalized absorption spectrum of NiB and phosphorescence emission spectrum of **SE-1**. b) Fluorescence spectrum of **SE-1**/NiB (0.5 wt% PR/0.01 wt% **1**/0.004 wt% NiB) under different strain during the tensile (λ_{ex} = 470 nm). c) The reversibility of fluorescence switching of **SE-1**/NiB under 100% and 400% strain (λ_{ex} = 470 nm). d) The fluorescence intensity changes at 533 and 670 nm of **SE-1**/NiB upon alternating 100% and 400% strain (λ_{ex} = 470 nm).

achieved mechano-induced ET with excellent fatigue resistance by doping energy acceptor NiB. This study extends the inherent reversible advantage of slide-ring cross-linkers to the mechanochromic materials and provides a facile method for the construction of a reversible mechanical response supramolecular elastomer with fatigue resistance.

Supporting Information

Supporting Information is available from the Wiley Online Library or from the author.

Acknowledgements

This work was financially supported by the National Natural Science Foundation of China (grant nos. 22131008 and 21971127). The authors thank the Fundamental Research Funds for the Central Universities and the Haihe Laboratory of Sustainable Chemical Transformations for financial support.

Conflict of Interest

The authors declare no conflict of interest.

Data Availability Statement

The data that support the findings of this study are available from the corresponding author upon reasonable request.

Keywords

cyclodextrin, mechanochromic, polyrotaxane, supramolecular elastomers

Received: November 26, 2022
Revised: December 29, 2022
Published online:

[1] C. Liu, N. Morimoto, L. Jiang, S. Kawahara, T. Noritomi, H. Yokoyama, K. Mayumi, K. Ito, *Science* **2021**, *372*, 1078.
[2] S. Choi, T.-W. Kwon, A. Coskun, J. W. Choi, *Science* **2017**, *357*, 279.

© 2023 Wiley-VCH GmbH

21951071, 0, Downloaded from https://onlinelibrary.wiley.com/doi/10.1002/adom.202202828 by Nankai University, Wiley Online Library on [10/02/2023]. See the Terms and Conditions (https://onlinelibrary.wiley.com/terms-and-conditions) on Wiley Online Library for rules of use; OA articles are governed by the applicable Creative Commons License

[3] a) R. Du, Q. Jin, T. Zhu, C. Wang, S. Li, Y. Li, X. Huang, Y. Jiang, W. Li, T. Bao, P. Cao, L. Pan, X. Chen, Q. Zhang, X. Jia, *Small* **2022**, *18*, 2200533; b) Y. Jiang, Z. Zhang, Y.-X. Wang, D. Li, C.-T. Coen, E. Hwaun, G. Chen, H.-C. Wu, D. Zhong, S. Niu, W. Wang, A. Saberi, J.-C. Lai, Y. Wu, Y. Wang, A. A. Trotsyuk, K. Y. Loh, C.-C. Shih, W. Xu, K. Liang, K. Zhang, Y. Bai, G. Gurusankar, W. Hu, W. Jia, Z. Cheng, R. H. Dauskardt, G. C. Gurtner, J. B. H. Tok, K. Deisseroth, et al., *Science* **2022**, *375*, 1411.

[4] L. Li, Q. Lin, M. Tang, E. H. R. Tsai, C. Ke, *Angew. Chem., Int. Ed.* **2021**, *60*, 10186.

[5] a) Z. Liu, Y. Liu, *Chem. Soc. Rev.* **2022**, *51*, 4786. b) X. Chen, H. K. Bisoyi, X.-F. Chen, X.-M. Chen, S. Zhang, Y. Tang, G. Zhu, H. Yang, Q. Li, *Matter* **2022**, *5*, 3883.

[6] a) B. Hetayothin, R. A. Cabaniss, F. D. Blum, *Macromolecules* **2017**, *50*, 2092; b) G. Liu, C. Zhou, W. L. Teo, C. Qian, Y. Zhao, *Angew. Chem., Int. Ed.* **2019**, *58*, 9366; c) G. Gao, G. Du, Y. Sun, J. Fu, *ACS Appl. Mater. Interfaces* **2015**, *7*, 5029.

[7] a) L. Chen, X. Sheng, G. Li, F. Huang, *Chem. Soc. Rev.* **2022**, *51*, 7046; b) X. Zhang, K. Liu, J. Zhao, Z. Zhang, Z. Luo, Y. Guo, H. Zhang, Y. Wang, R. Bai, D. Zhao, X. Yang, Y. Liu, X. Yan, *J. Am. Chem. Soc.* **2022**, *144*, 11434; c) S. Huang, Y. Shen, H. K. Bisoyi, Y. Tao, Z. Liu, M. Wang, H. Yang, Q. Li, *J. Am. Chem. Soc.* **2021**, *143*, 12543.

[8] H. Gotoh, C. Liu, B. Imran Abu, M. Hara, T. Seki, K. Mayumi, K. Ito, Y. Takeoka, *Sci. Adv.* **2018**, *4*, eaat7629.

[9] a) L. Feng, S.-S. Jia, Y. Chen, Y. Liu, *Chem. - Eur. J.* **2020**, *26*, 14080; b) S. Wang, Y. Chen, Y. Sun, Y. Qin, H. Zhang, X. Yu, Y. Liu, *Commun. Mater.* **2022**, *3*, 2.

[10] a) A. Bin Imran, K. Esaki, H. Gotoh, T. Seki, K. Ito, Y. Sakai, Y. Takeoka, *Nat. Commun.* **2014**, *5*, 5124; b) Q. Lin, L. Li, M. Tang, S. Uenuma, J. Samanta, S. Li, X. Jiang, L. Zou, K. Ito, C. Ke, *Chem* **2021**, *7*, 2442; c) Y. Zhang, C. Zhang, Y. Chen, J. Yu, L. Chen, H. Zhang, X. Xu, Y. Liu, *Adv. Opt. Mater.* **2022**, *10*, 2102169; d) W.-Z. Li, X. Li, F. Yang, Y. Chen, Y.-X. Wang, *Macromol. Rapid Commun.* **2022**, *43*, 2200082; e) C.-Y. Shi, Q. Zhang, C.-Y. Yu, S.-J. Rao, S. Yang, H. Tian, D.-H. Qu, *Adv. Mater.* **2020**, *32*, 2000345.

[11] a) M. M. Caruso, D. A. Davis, Q. Shen, S. A. Odom, N. R. Sottos, S. R. White, J. S. Moore, *Chem. Rev.* **2009**, *109*, 5755; b) J. Li, C. Nagamani, J. S. Moore, *Acc. Chem. Res.* **2015**, *48*, 2181; c) T. Han, L. Liu, D. Wang, J. Yang, B. Z. Tang, *Macromol. Rapid Commun.* **2021**, *42*, 2000311; d) J. Yang, J. Qin, P. Geng, J. Wang, M. Fang, Z. Li, *Angew. Chem., Int. Ed.* **2018**, *57*, 14174. e) H. K. Bisoyi, Q. Li, *Chem. Rev.* **2022**, *122*, 4887.

[12] a) Y. Dong, A. N. Ramey-Ward, K. Salaita, *Adv. Mater.* **2021**, *33*, 2006600; b) C. Yang, Z. Suo, *Nat. Rev. Mater.* **2018**, *3*, 125; c) R. Merindol, G. Delechiave, L. Heinen, L. H. Catalani, A. Walther, *Nat. Commun.* **2019**, *10*, 528; d) C. Calvino, A. Guha, C. Weder, S. Schrettl, *Adv. Mater.* **2018**, *30*, 1704603; e) Q. Wang, Q. Zhang, Q.-W. Zhang, X. Li, C.-X. Zhao, T.-Y. Xu, D.-H. Qu, H. Tian, *Nat. Commun.* **2020**, *11*, 158; f) Z. Li, P. Liu, X. Ji, J. Gong, Y. Hu, W. Wu, X. Wang, H.-Q. Peng, R. T. K. Kwok, J. W. Y. Lam, J. Lu, B. Z. Tang, *Adv. Mater.* **2020**, *32*, 1906493; g) X.-M. Chen, X.-F. Hou, H. K. Bisoyi, W.-J. Feng, Q. Cao, S. Huang, H. Yang, D. Chen, Q. Li, *Nat. Commun.* **2021**, *12*, 4993; h) Y. Huang, H. K. Bisoyi, S. Huang, M. Wang, X.-M. Chen, Z. Liu, H. Yang, Q. Li, *Angew. Chem., Int. Ed.* **2021**, *60*, 11247.

[13] a) H. Hu, X. Cheng, Z. Ma, R. P. Sijbesma, Z. Ma, *J. Am. Chem. Soc.* **2022**, *144*, 9971; b) H. Qian, N. S. Purwanto, D. G. Ivanoff, A. J. Halmes, N. R. Sottos, J. S. Moore, *Chem* **2021**, *7*, 1080. c) Z. Liu, H. K. Bisoyi, Y. Huang, M. Wang, H. Yang, Q. Li, *Angew. Chem., Int. Ed.* **2022**, *61*, e202115755;

[14] a) Y. Jia, S. Wang, W.-J. Wang, B.-G. Li, S. Zhu, *Macromolecules* **2019**, *52*, 7920; b) M. Horst, J. Yang, J. Meisner, T. B. Kouznetsova, T. J. Martínez, S. L. Craig, Y. Xia, *J. Am. Chem. Soc.* **2021**, *143*, 12328; c) Y. Sun, W. J. Neary, Z. P. Burke, H. Qian, L. Zhu, J. S. Moore, *J. Am. Chem. Soc.* **2022**, *144*, 1125; d) B. A. Versaw, T. Zeng, X. Hu, M. J. Robb, *J. Am. Chem. Soc.* **2021**, *143*, 21461.

[15] a) A. D. Das, G. Mannoni, A. E. Früh, D. Orsi, R. Pinalli, E. Dalcanale, *ACS Appl. Polym. Mater.* **2019**, *1*, 2990; b) T. Muramatsu, Y. Okado, H. Traeger, S. Schrettl, N. Tamaoki, C. Weder, Y. Sagara, *J. Am. Chem. Soc.* **2021**, *143*, 9884.

[16] K. Imato, R. Yamanaka, H. Nakajima, N. Takeda, *Chem. Commun.* **2020**, *56*, 7937.

[17] a) Y. Sagara, H. Traeger, J. Li, Y. Okado, S. Schrettl, N. Tamaoki, C. Weder, *J. Am. Chem. Soc.* **2021**, *143*, 5519; b) J. Chen, A. W. Ziegler, B. Zhao, W. Wan, A. D. Q. Li, *Chem. Commun.* **2017**, *53*, 4993.

[18] L. Yu, R. Zhao, N. Wang, S. Feng, X.-D. Xu, *ACS Appl. Polym. Mater.* **2021**, *3*, 3623.

[19] H. Traeger, Y. Sagara, D. J. Kiebala, S. Schrettl, C. Weder, *Angew. Chem., Int. Ed.* **2021**, *60*, 16191.

[20] A. E. Früh, F. Artoni, R. Brighenti, E. Dalcanale, *Chem. Mater.* **2017**, *29*, 7450.

© 2023 Wiley-VCH GmbH

21951071, 0, Downloaded from https://onlinelibrary.wiley.com/doi/10.1002/adom.202202828 by Nankai University, Wiley Online Library on [10/02/2023]. See the Terms and Conditions (https://onlinelibrary.wiley.com/terms-and-conditions) on Wiley Online Library for rules of use; OA articles are governed by the applicable Creative Commons License